



New alginate acid–atenolol microparticles for inhalatory drug targeting



Nazareth Eliana Ceschan^{a,b}, Verónica Bucalá^{a,b}, María Verónica Ramírez-Rigo^{a,c,*}

^a Planta Piloto de Ingeniería Química (PLAPIQUI), CONICET, Universidad Nacional del Sur (UNS), Camino La Carrindanga Km 7, 8000 Bahía Blanca, Argentina

^b Departamento de Ingeniería Química, UNS, Avenida Alem 1253, 8000 Bahía Blanca, Argentina

^c Departamento de Biología, Bioquímica y Farmacia, UNS, San Juan 670, 8000 Bahía Blanca, Argentina

ARTICLE INFO

Article history:

Received 10 December 2013

Received in revised form 19 March 2014

Accepted 18 April 2014

Available online 27 April 2014

Keywords:

Powder engineering

Spray drying

Polyelectrolyte–drug complex

Solid-state characterization

Inhalatory route

ABSTRACT

The inhalatory route allows drug delivery for local or systemic treatments in a noninvasively way. The current tendency of inhalable systems is oriented to dry powder inhalers due to their advantages in terms of stability and efficiency. In this work, microparticles of atenolol (AT, basic antihypertensive drug) and alginate acid (AA, acid biocompatible polyelectrolyte) were obtained by spray drying. Several formulations, varying the relative composition AT/AA and the total solid content of the atomized dispersions, were tested. The powders were characterized by: Fourier Transform Infrared Spectroscopy, Differential Scanning Calorimetry and Powder X-ray Diffraction, while also the following properties were measured: drug load efficiency, flow properties, particles size and density, moisture content, hygroscopicity and morphology. The ionic interaction between AA and AT was demonstrated, then the new chemical entity could improve the drug targeting to the respiratory membrane and increase its time residence due to the mucoadhesive properties of the AA polymeric chains. Powders exhibited high load efficiencies, low moisture contents, adequate mean aerodynamic diameters and high cumulative fraction of respirable particles (lower than 10 μm).

© 2014 Elsevier B.V. All rights reserved.

1. Introduction

The inhalatory route allows both local and systemic drug administration [1]. This requires an efficient targeting of the particles or droplets containing the active ingredient to the action or absorption site [2].

The current tendency of inhalable systems is oriented to dry powder inhalers, which have competitive advantages in terms of stability and efficiency over nebulization systems or metered doses inhalers [3]. However, for dry powder inhalers a rational design of the particulate system is required. The characteristics of the powder (shape, size, density, porosity, surface charge, among others) strongly affect the particles' aerosolization and deposition, as well as the formulation release and residence time at the action or absorption site [2]. Therefore, the particle system properties modify significantly the biopharmaceutical performance of the formulation [4].

Spray drying is a technology for producing particulate systems with controlled quality by a suitable selection of the fluid feed composition and process operating conditions [5]. In this technique, a liquid feed is atomized aided by pressurized air in devices called binary nozzles. Fine droplets formed during atomization are dried by means of hot air. The spray drier can operate in either co-current or counter-current mode, while the drying air flow can be promoted by negative or positive

pressure systems. Finally, cyclones facilitate the dried powder collection [6,7]. Spray drying is currently selected to develop inhalable particles because it is a scalable continuous technology, able to process a variety of liquid feeds (solutions, dispersions and emulsions) based on materials of different nature [8].

The formulation of a bioactive substance in inhalable polymeric particles could modulate residence time, release rate and/or absorption of this molecule in the respiratory membrane [9]. Particularly, the combination of acid or basic drugs with polyelectrolytes of opposite charge leads to new chemical entities with physicochemical, pharmaceutical and/or biopharmaceutical properties different from their precursors [10]. The polyelectrolytes are polymers constituted by monomers that have ionizable functional groups. These groups dissociate in aqueous solutions [11].

Inhalatory particulate materials based on polyelectrolyte–drug complexes obtained by spray drying were reported for local infections [12,13], gene therapy or gene replacement [14]. For these particular treatments, cationic polymers such as chitosan, polylysine and cationic dendrimers were combined with antineoplastic drugs [15], DNA plasmids [16] and oligonucleotides [17]. For the same applications, anionic polyelectrolytes such as dextran, alginate acid and poly-lactic-co-glycolic-acid were associated to fluoroquinolonic antibiotics [18], rifampicin, isoniazid and perfenazine [19], and peptides and proteins with net positive charge [20]. In addition, inter-polyelectrolyte complexes were reported for inhalatory applications. For example, powders constituted by chitosan–alginate acid to deliver fluoroquinolonic antibiotics [21] and polylysine–alginate acid to carry oligonucleotides [22] were developed.

* Corresponding author at: Planta Piloto de Ingeniería Química (PLAPIQUI), CONICET, Universidad Nacional del Sur (UNS), Camino La Carrindanga Km 7, 8000 Bahía Blanca, Argentina. Tel.: +54 291 486 1700x265; fax: +54 291 486 1600.

E-mail address: vrrigo@plapiqui.edu.ar (M.V. Ramírez-Rigo).

The particles of polyelectrolyte–drug complexes obtained by spray drying reported in the literature were mainly described as spherical or rounded, belonging to unimodal populations and with suitable aerodynamic diameters for inhalatory administration. Some porous particles were obtained when volatile solvents were used as feed [6]. The products could be charged or un-charged depending on the neutralization degree [23]. Although these contributions are interesting, the characterization of the solid state of these materials and the relationships between the process and the product quality are fields that require to be explored.

The available studies were mainly focused on demonstrating that these new materials target bioactive molecules to the action or absorption sites and modify properties such as DNA compaction and transfection, mucosal adherence, particle mucociliary clearance, stability, dissolution rate and permeability of drugs [10,24]. Accordingly, bioavailability of active ingredients administered as part of particulate complexes is improved respect to that achieved by administration of the pure active substances [9].

Due to the reported advantages of polyelectrolyte–drug powders, drugs recognized as safe and effective, but with some unfavourable physicochemical or biopharmaceutical properties, are good candidates to be loaded on a polyelectrolyte.

There are many therapeutic groups that could be favoured by this technological approach, among others, cardioselective drugs [25]. Atenolol (AT) is a beta-blocker drug [26] used for the treatment of hypertension. It reduces heart rate (negative chronotropic effect) and heart contractile force (negative inotropic effect). AT is formulated in tablets or parenteral solutions. Orally administered AT exhibits low bioavailability (40–50%) due to its poor intestinal absorption [27] through paracellular pathway [28]. Parenteral solutions are only used when a fast onset of action is required, such as in early intervention of myocardial infarction [29]. However, needle pain and infection risk are some disadvantages of this administration route [30].

AT is known to have adequate permeation in human airway epithelial cell line Calu-3 and in isolated perfused lung by passive diffusion mechanisms [31]. Also, being beta-1-cardiac selective, AT presents no bronchodilator effect [26,32]. With the aim of improving the biopharmaceutical performance of this drug, the systemic administration of inhaled AT emerges as an alternative (non-invasive) to the oral route. This strategy was approached by Ravinowitz and Zaffaroni through the development of liquid inhalation formulations of antihypertensive active ingredients to be administered by vaporization and condensation processes [33].

Taking into account of advantages of the dry powder inhalers over liquid formulations and the particular properties of polyelectrolyte–drug materials, the design of a particulate system, in a size range suitable to target AT to the respiratory membrane, is an interesting challenge. Based on the capacity of AT to interact with anionic polyelectrolytes [34, 35], alginic acid (AA) was selected for binary AT–AA formulations. AA is a mucoadhesive polyelectrolyte, being then an attractive material to increase the formulation residence time on the site of absorption. It is widely used in drug delivery devices and it was also proposed for inhalatory administration of local or systemic drugs [36–38].

The main goal of this work is to develop a new material to administrate AT by the respiratory route. To this aim, AA–AT microparticles obtained by spray drying were analysed at molecular, particulate and bulk level in order to identify the relationship between the feed formulation and the key powder properties that make the materials suitable for inhalatory drug delivery.

2. Materials and methods

2.1. Materials

AA from Brown Algae (analytical grade, Sigma, Saint Louis, United States), AT (pharmaceutical grade, Parafarm, Saporiti, Buenos Aires, Argentina), potassium bromide (spectroscopic grade, Merck, Darmstadt, Germany), lactose monohydrate (pharmaceutical grade, Parafarm,

Saporiti, Buenos Aires, Argentina) with particle sizes between 70 and 140 mesh sieves (ASTM) and distilled water were used.

AT is a basic drug (pKa 9.6, Fig. 1a), while AA is an acid biocompatible polyelectrolyte (pKa 3.5, Fig. 1b). AA, a linear polymer, is obtained from the cell wall of brown algae. It consists of guluronic and mannuronic acid subunits linked with glycosidic bonds. AA is known to be safe, biocompatible, biodegradable, economic and insoluble but dispersible in water.

2.2. Determination of number of equivalents of carboxylic groups and sodium content in AA samples

Acidic groups available to be neutralized by the drug and sodium content of the raw material were evaluated due to their relevance in the formulation of the feed dispersions.

The number of equivalents of carboxylic groups per AA gramme was determined by potentiometric titration using NaOH (0.00993 N) solution. The sodium content was assayed by flame atomic emission (AAAnalyst 700, Atomic Absorption Spectrometer, Perkin Elmer, Massachusetts, United States).

The evaluated material had 4.55×10^{-3} equivalents per AA gramme and its sodium content was low (2.26 mg/kg of AA).

2.3. Dispersion preparation and characterization

To establish relationships between the properties of particles obtained by spray drying and the feed composition, dispersions with different ratios AT/AA and total solid contents were prepared (see Table 1). The percentages that are assigned to the sample names indicate the total solid concentration, while for the binary formulations the subscripts refer to the percentage of carboxylic acid groups of AA neutralized by AT.

For a set of samples, the AA (which is a viscosity increasing agent) was dispersed under stirring in distilled water (1% w/v) and AT (as a powder) was incorporated in the amount required to neutralize 25, 50 and 75% of the AA acid groups. The samples were identified as (AA–AT)₂₅ 1.3%, (AA–AT)₅₀ 1.6% and (AA–AT)₇₅ 1.9%, all of them had the same amount of AA (2 g) and the AT content varied according to the neutralization degree. Keeping the AA mass while AT is varied allows studying changes in the feed viscosity associated to the interaction polymer–drug.

To compare the properties of the powder obtained by processing a (AA–AT)₅₀ 1.6% dispersion with those of the materials produced by using pure AT and AA, the AT 0.6% solution and the AA 1% dispersion were also prepared. According Table 1 these samples had the same amount of pure compounds than the (AA–AT)₅₀ 1.6% dispersion, being then possible the comparison between the powders obtained by atomizing the three mentioned formulations.

To study the influence of the total solid content at constant neutralization degree, dispersions with the adequate AT amount to neutralize the 50% of the AA acid groups were prepared from AA 2.5 and 5% w/v suspensions, which were named as (AA–AT)₅₀ 4% and (AA–AT)₅₀ 8%, respectively (Table 1). These samples can be compared with the above introduced (AA–AT)₅₀ 1.6% formulation.

To evaluate the effect of the feed composition on the process yield, dispersions with different neutralization degrees but with the same total solid content were prepared, they were named as (AA–AT)₂₅ 1.6% and (AA–AT)₇₅ 1.6% (Table 1). For comparative purposes, the dispersion AA 1.6% and the solution AT 1.6% were also prepared (Table 1).

For all the samples listed in Table 1, the volume selected for the solutions/dispersions preparation was 200 mL.

The following dispersions/solutions physicochemical properties were measured:

- pH, by using a pH meter Orion 410A, Cole Parmer, Vermon Hills, United States.

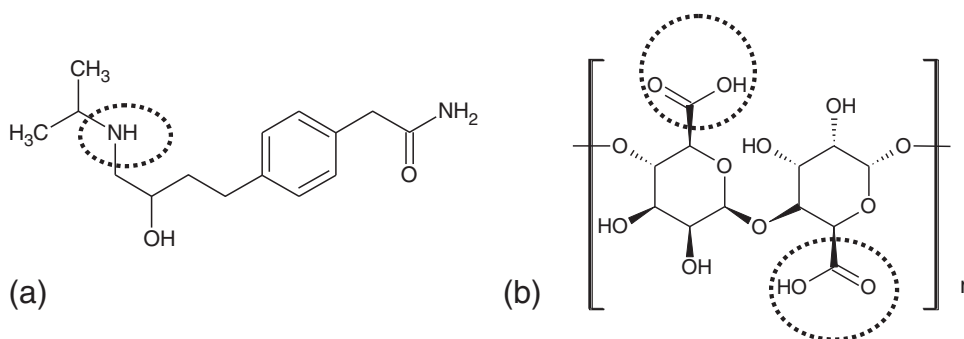


Fig. 1. Structural formula of (a) AT and (b) AA (a mannuronic acid subunit linked to a guluronic acid subunit as example) showing their basic or acidic functional groups.

- Kinematic viscosity, at 25 °C employing a capillary Cannon–Fenske Routine-type viscometer (Tube size 100, IVA), Cannon Instrument Company, State College, United States.
- Density, at 25 °C using a pre-calibrated glass pycnometer (Gay–Lussac type). This property was only evaluated for the dispersion of highest viscosity: (AA–AT)₅₀ 8%. This data was used to calculate the dynamic viscosity:

$$\eta_{dynamic} = \eta_{kinematic} \rho \quad (1)$$

where $\eta_{dynamic}$ and $\eta_{kinematic}$ are the dynamic and kinematic viscosity, respectively, and ρ is the fluid density.

- Electrokinetic potential, by means of Zetasizer 3000, Malvern Instruments, Worcestershire, United Kingdom. For electrokinetic potential determinations and due to equipment requirements, samples were diluted to a final concentration of 0.1% w/v. The information relative to the physical stability of the systems provided by this experiment is independent of the concentration, giving a measurement of charged particle repulsion [39].
- Final AT amount in dispersions, this composition was confirmed by UV–spectrophotometry (UV–160A, Spectrophotometer, Shimadzu, Burladingen, Germany) at 274.6 nm. This analytical method was proposed by USP [40] and Florey [41] for pure AT. In addition the AA did not affect the AT quantification by UV [35], therefore this method can be applied for the characterization of binary dispersions.

All the above mentioned experiments were made by triplicate.

2.4. Spray drying

Dispersions and solutions were atomized under constant magnetic stirring (condition particularly relevant for pure AA dispersions which are physically unstable) in a negative pressure laboratory scale spray drying equipment (Mini Spray Dryer B-290, BÜCHI, Flawil, Switzerland).

A two-fluid nozzle with a cap-orifice diameter of 0.5 mm was used. Operating conditions were selected accordingly to data reported for spray drying of pure sodium alginate [20,42,38,43–45]: air inlet temperature (co-current) 140 °C, atomization air flow rate 601 L/h, liquid feed flow rate 20% (6 mL/min) and drying air flow rate 35 m³/h. The collected powder was weighed, packed in sealed amber bottles and stored for further characterization.

The (AA–AT)₇₅ 1.9% (Table 1) dispersion was processed using the above mentioned operating conditions and also by changing the atomization air flow rate from 601 L/h (fixed value for all samples) to 742 L/h, the product obtained under this new condition was named (AA–AT)₇₅ 1.9%^b. The atomization air flow rate was disturbed to analyse the effect of the atomized droplet size on the quality of the product [46].

The process yield was calculated as the ratio of the weight of product collected after spray drying to the initial amount of solids used to prepare the aqueous dispersions or solutions.

2.5. Particulate system characterization

2.5.1. Moisture content

Moisture content of the product was determined immediately after the spray-drying process in a halogen moisture analyser (MB45, Ohaus, Pine Brook, United States). About 500 mg of powder was heated up to 105 °C until the weight change was less than 1 mg in 60 s.

2.5.2. Drug loading efficiency

AT mass concentration of the binary spray-dried product was determined by UV–spectrophotometry. The powders were dispersed in distilled water and the concentration of AT in the dispersion was measured at 274.6 nm. The drug loading efficiency was reported as gramme of the drug in 1 g of the sample.

Table 1

Composition, viscosity and pH of suspensions and solutions for spray drying.

Sample	Theoretical formulation				Experimental dispersion properties		
	AA (g)	AT (g)	AA concentration (%w/v)	Total solids (%w/v)	Relative composition ($\frac{g_{AT}}{g_{AA}}$)	Viscosity (mm ² /s)	pH
(AA–AT) ₂₅ 1.3%	2.00	0.61	1.0	1.3	0.27 ± 0.01	7.24 ± 0.04	2.92 ± 0.03
(AA–AT) ₅₀ 1.6%	2.00	1.21	1.0	1.6	0.57 ± 0.01	7.00 ± 0.05	3.04 ± 0.01
(AA–AT) ₇₅ 1.9%	2.00	1.82	1.0	1.9	0.85 ± 0.03	4.60 ± 0.04	4.11 ± 0.02
(AA–AT) ₅₀ 4%	5.00	3.03	2.5	4.0	0.56 ± 0.02	23.90 ± 0.34	3.01 ± 0.01
(AA–AT) ₅₀ 8%	10.00	6.06	5.0	8.0	0.59 ± 0.02	54.14 ± 0.42	3.00 ± 0.03
(AA–AT) ₂₅ 1.6%	2.47	0.75	1.2	1.6	0.29 ± 0.01	7.02 ± 0.07	2.98 ± 0.02
(AA–AT) ₇₅ 1.6%	1.68	1.52	0.8	1.6	0.85 ± 0.02	4.18 ± 0.08	4.26 ± 0.02
AA 1%	2.00	–	1.0	1.0	–	–	2.77 ± 0.02
AA 1.6%	3.21	–	1.6	1.6	–	–	2.54 ± 0.05
AT 0.6%	–	1.21	–	0.6	–	–	10.00 ± 0.04
AT 1.6%	–	3.21	–	1.6	–	–	11.20 ± 0.04

Subscripts 25, 50 and 75 represent the degree of AA neutralization while the percentages indicate the total solid content

2.5.3. Infrared spectroscopy associated to Fourier Transform (FT-IR), Differential Scanning Calorimetry (DSC) and Powder X-Ray Diffraction (PXRD) characterization

- FT-IR. Samples were studied in 1% w/w potassium bromide compacts using a FT-IR instrument (Nexus FT, Termonicolet, Maryland, United States). The spectra resulted was the average of 32 scans and 4% resolution. Samples and potassium bromide were dried at 105 °C until constant weight prior to testing.
- DSC. Thermograms were obtained (Pyris 1, Perkin Elmer, Massachusetts, United States) from samples placed in closed aluminium pans under nitrogen atmosphere flowing at 40 mL/min. To determine DSC curves, the temperature axis and the cell constant were previously calibrated with indium. 5 mg samples were heated from 30 to 180 °C at 10 °C/min, then they were cooled down to 30 °C and finally temperature was raised up to 180 °C (at 10 °C/min). Glass transition temperature (T_g) of products (AA–AT)_x 1.3–1.9%, as-received AA (AA_{op}), AA 1% and the physical mixture of AA and AT was estimated by triplicate using the half ΔC_p method [5]. Melting temperature and enthalpy (T_{onset} and ΔH_m) of as-received AT (AT_{op}), AT 0.6% and the drug in physical mixture were also determined.
- PXRD. Crystallographic patterns were recorded between the angles (2θ) 5 and 65° (Rigaku, Geigerfleck, Tokyo, Japan), using an anodic Copper tube with monochromator operated at 35 kV y 15 mA. The step measurement was 0.04° and step time was 0.8 s. Crystallinity loss and disorder degree of the samples were evaluated using Scherrer equation [47] through Jade Software (Jade Software Corporation, [48]). Briefly, Scherrer equation relates the size of submicroscopic particle, or crystal, in a solid with the broadening of a peak in an X-ray diffraction diagram, indicating the crystalline packet size responsible for a peak signal, which can be stated as:

$$\tau = \kappa\lambda/\beta \cos\theta \quad (2)$$

where τ is the mean size of crystalline or organized part, κ is a shape factor, λ wave longitude of X radiation, β is the Full Width at Half Maximum (FWHM) and θ is the Bragg angle.

2.5.4. Particle morphology and size distribution

Particle size distribution was measured by laser diffraction using the dry powder method (LA 950 V2, Horiba, Kyoto, Japan). The spray-dried powders were dispersed in lactose (with a known particle size distribution) in a proportion lactose:sample 4:1 to improve the sample flow from the feed hopper to the measuring cell. The volume average diameter of lactose differs substantially from the average size of the powder obtained by spray drying. As a consequence, bimodal distributions, with two modes perfectly distinguishable were obtained allowing an accurate granulometry measurement. Complementarily, particle size distributions were evaluated for pure AA, AT and lactose as they were received from suppliers. Size is reported as mean volumetric diameter (D_{43}) and distribution width is informed as *span*. Span index is calculated as shown in Eq. (3).

$$Span = (D_{90} - D_{10})/D_{50} \quad (3)$$

where D_{90} , D_{50} and D_{10} are the diameters where the 90%, 50% and 10% of the population lie below each value, respectively. A distribution can be considered relatively narrow if the *span* value is less than 2 [49].

Particle morphology was evaluated through Scanning Electron Microscopy (SEM). Samples were metalized with gold (Sputter Coater 91000, PELCO, TellPella, Canada) and they were observed and photographed using an EVO 40-XVP, LEO scanning electron microscope (Oberchoken, Germany).

2.5.5. Particle and bulk density determination

The sample or skeletal density of the spray-dried products was determined by nitrogen adsorption (Nova 1200e, Quantachrome Instruments, Florida, United States). A sample of 1 g was placed in a precalibrated cell and its volume was determined by the intrusion of nitrogen. The sample density was calculated as the solid mass divided by the volume of the particle excluding the open pores. For very porous particles and well-connected pores the sample density can be assumed to be close to the solid density, while for non-porous particles the sample density represents the particle density.

In order to determine bed densities of the spray-dried samples, the powder was gently poured into a 10 cm³ graduated cylinder. Bulk density (D_{bulk}) was calculated as the ratio of the weight (g) of the sample contained in the cylinder to the volume occupied (10 cm³). Tap density (D_{tap}) was estimated by tapping the cylinder until no measurable change in volume was noticed. All determinations were made by triplicate. Carr Index (C, Eq. (4)) was evaluated:

$$C = \left(D_{tap} - D_{bulk} \right) 100 / D_{tap} \quad (4)$$

Carr indexes of 10% indicate an excellent flow, between 10 and 15% show good fluency, in 16–20% range powder's flow is fair, between 21 and 25% flow is considered passable, in 26–31% range powder's flow is poor, between 32 and 37 is very poor and bigger than 38% is very, very poor [40].

Since the powders clogged the funnel recommended by USP to measure the repose angle, an alternative method [50,51] was employed. Briefly, a glass cylinder was placed above a graph paper located on a flat horizontal surface and it was filled with 2.5 g of sample. Then, the cylinder was lifted and the height (h) and radius (r) of the conical pile formed were measured. The tangent of the angle of repose is given by the h/r ratio. All the measurements were made with a calibre. If the angle of repose is less than 25° the flow is said to be excellent, between 25 and 30° the powder flow is good, between 30 and 40° the flow is considered regular, in the 40–45° range the flow is poor and values higher than 50° indicate that powder have very poor flow properties [51].

2.5.6. Hygroscopicity

Moisture uptake of products was evaluated at 25 °C and 75% relative humidity (RH), following the ASTM D5032-97 norm [52]. Samples of 100 mg were stored in hermetic recipients containing appropriated glycerol–water mixture to control RH for 15 days. The samples were reweighed and the weight increase was associated to the water adsorption.

2.5.7. Aerodynamic diameter estimation

Particle aerodynamic diameter (D_{aer}) can be estimated by the following formula [53]:

$$D_{aer} = D_{43} \sqrt{D_p} \quad (5)$$

where D_p is the particle density and D_{43} is the particle volumetric mean diameter (which is establish by laser diffraction). In this work, the sample or skeletal densities (estimated from the nitrogen adsorption experiments) are available. As above mentioned, for non-porous particles the sample density becomes equal to the particle porosity. For porous powders, the sample density will be higher than the particle one. Therefore, the aerodynamic diameters calculated based on sample density are overestimated. In other words, if the calculated aerodynamic diameters (approximated values) are adequate for inhalation, surely the particles will be suitable for inhalatory systems.

3. Results and discussion

3.1. Feed AA–AT aqueous dispersions characterization

3.1.1. Ionic pair formation

When an anionic polyelectrolyte is combined with basic drugs (D) in an aqueous medium, ionic pairs between them are generated according with the Eqs. ((6)–(8)).



where R-COOH and R-COO[−] represent a polyelectrolyte with carboxylic or carboxylate groups respectively; D and DH⁺ represent the unprotonated and protonated D species and [RCOO[−]DH⁺] represents the ionic pair. Eq. (8) is known as counterion condensation in polyelectrolyte solutions [54,55].

The equilibrium properties of polyelectrolyte-D dispersions were described for several anionic polymers, among others, carbomer [56], hyaluronic acid [57], the acid form of carboxymethylcellulose [58] and alginate acid [35]. It was demonstrated that ionic pairs are in high proportion in water. On the other hand, those ionic pairs when exposed to physiological medium tend to dissociate, releasing the drug by ionic exchange. Particularly, Ramírez Rigo et al. [35] observed this behaviour for (AA–AT)₁₀₀ dispersion (11.3% of solid content) when drug release was evaluated in water and 0.9% NaCl solution at 37 °C. These results allow postulating that spray drying of AA–AT aqueous dispersions could conduct to ionic complexes in the solid state. Moreover, according to Ramírez Rigo et al. [35], a AA–AT solid product in contact with physiological medium would wet, swell and release the drug, being then available for absorption. Based on the previous results, the dispersions listed in Table 1 were prepared to explore the feasibility to obtain ionic complexes by spray drying.

3.1.2. pH of the dispersions

As it can be seen in Table 1, the addition of AT to the AA (as expected from the reactions above mentioned) raised the pH from 2.54 or 2.77 (samples named as AA 1 and 1.6%) to values between 2.98 and 4.26 (for the (AA–AT)_x 1.3–8% dispersions) in agreement with the percentage of carboxylic groups of AA neutralized ($x = 25\text{--}75\%$).

3.1.3. Physical stability

Pure AA dispersions prepared tended to settle down quickly under repose [59]. On the other hand, all the AA–AT dispersions did not show evidence of phase separation. To prove the physical stability of these binary systems, they were appropriately diluted and their electrokinetic potentials were determined. The measured values were: -37.23 ± 0.52 , -42.53 ± 0.29 and -45.12 ± 0.26 mV for (AA–AT)₂₅, (AA–AT)₅₀ and (AA–AT)₇₅, respectively. These high negative electrokinetic potentials indicated good stability [39] considering that -30 mV is the general limit reported [60]. The polymeric chains partially neutralized by AT that composed the dispersed phase tended to repel each other in a sufficient extent to prevent aggregation. The increment of the electrokinetic potential with the proportion of AT in the dispersion could be associated to the increase in the ionization degree of the free-carboxylic groups of the macromolecule due to the rise of pH near its pKa value.

On these bases, the AA–AT dispersions can be considered suitable for their atomization in a continuous process.

3.1.4. Viscosity

In spray drying, the viscosity of the feed is recognized as an important factor that influences droplet size, process yield and product size and morphology. For this reason, the kinematic viscosities of the feed binary dispersions were determined. The viscosity values were between 4.18 and 54.14 mm²/s (see Table 1). The results indicate that both the solid content and the AT/AA ratio affect the dispersion viscosity. Even in the series that maintained constant the concentration of AA (viscosity increasing agent), the (AA–AT)₇₅ 1.9% dispersion displayed lower viscosity than (AA–AT)₂₅ 1.3% and (AA–AT)₅₀ 1.6% dispersions. This behaviour could be related to the interaction between the polyelectrolyte and the drug that affects the charge density and chain conformation of the macromolecule [60].

The maximum dynamic viscosity for a feed to be adequately atomized by spray drying was reported as 250 Pa·s [42,61]. The highest viscosity exhibited by dispersions was 55.63 Pa·s for (AA–AT)₅₀ 8%. According to this, all dispersions are suitable for atomization.

3.1.5. Experimental composition

In order to compare the AT concentration in the spray-dried powders, the AT/AA ratio in the dispersions were measured by UV. The experimental values reported in Table 1 are in good agreement with theoretical formulations. The observed small deviations are due to weighting process.

3.2. Spray-drying process

As shown in Table 2 outlet air temperatures were equal to or lower than 85 °C, thermal level at which AA and AT demonstrated to be chemically stable. In fact, temperatures higher than 200 °C are needed to degrade these compounds [62,63].

Drying the (AA–AT)_x 1.3–8% dispersions, the process yields (Table 2) laid between 45.84 and 72.70% and were acceptable values considering that a lab-scale spray dryer was used [64]. These yields were noticeably higher than the ones obtained when solutions/dispersions containing pure compounds were processed, this result indicates that the new chemical entities are more plausible to be processed by spray drying than their precursors.

Comparing samples with equal neutralization degree ($x = 25, 50$ or 75%), as a general trend, the higher dispersion solid content the higher process yield. This behaviour could be attributed to the lower droplet water amount in the more concentrated dispersions. This tendency was not followed only by the sample (AA–AT)₅₀ 8%, indeed its yield was 52.31% sensibly lower than the 72.40% value obtained by processing the (AA–AT)₅₀ 4% dispersion. The high viscosity of the (AA–AT)₅₀ 8% dispersion (which is the highest one of the studied set of samples) favoured the solid adhesion on the spray-dryer chamber wall, probably due to the droplet size dependence with viscosity (bigger droplets are more difficult to dry) [65,66].

For a given value of solid content (1.6% w/v), the process yield of formulations with different neutralization degrees were also analysed. The samples (AA–AT)_x 1.6% presented process yields of 58.69, 65.90 and 59.76% for neutralization degrees of 75, 50 and 25%, respectively. For this level of solid content, the neutralization degree did not strongly affect the process yield.

In summary, the feed solid concentration was the main variable that modify process yield of AA–AT dispersions with total solids between 1.3 and 4%.

3.3. Product characterization

3.3.1. Moisture content

The moisture contents of all powders obtained are listed in Table 2. For the (AA–AT)_x samples, the powder moisture ranged from 3.43 to 5.32%, values that are relatively low and indicate that drying of these materials using the selected operating conditions was efficient (see

Table 2
Outlet temperature and yield of the spray drying and residual moisture, relative composition and load efficiency of products.

Sample	T _{out} (°C)	Yield (%)	Residual moisture (%)	Relative composition (g _{AT} /g _{AA})	Load efficiency (g _{AT} /g _{solid})
(AA-AT) ₂₅ 1.3%	85.0 ± 0.0	58.72 ± 1.53	5.14 ± 0.86	0.54 ± 0.01	0.36 ± 0.01
(AA-AT) ₅₀ 1.6%	82.7 ± 0.6	65.90 ± 2.38	5.32 ± 0.98	0.91 ± 0.01	0.48 ± 0.01
(AA-AT) ₇₅ 1.9%	83.7 ± 0.6	67.40 ± 2.23	3.55 ± 0.01	1.72 ± 0.02	0.63 ± 0.02
(AA-AT) ₅₀ 4%	78.0 ± 1.2	72.70 ± 2.88	4.14 ± 0.08	0.98 ± 0.01	0.50 ± 0.01
(AA-AT) ₅₀ 8%	80.0 ± 1.8	52.31 ± 3.51	3.43 ± 0.46	1.38 ± 0.02	0.58 ± 0.02
(AA-AT) ₂₅ 1.6%	79.5 ± 0.7	59.76 ± 2.45	4.36 ± 0.41	0.39 ± 0.01	0.30 ± 0.01
(AA-AT) ₇₅ 1.6%	79.0 ± 1.4	58.69 ± 3.30	4.35 ± 0.05	1.13 ± 0.02	0.59 ± 0.02
(AA-AT) ₇₅ 1.9% ^b	80.2 ± 1.8	45.84 ± 2.64	3.95 ± 0.14	1.18 ± 0.01	0.62 ± 0.01
AA 1%	83.3 ± 0.5	18.14 ± 3.01	7.24 ^a	–	–
AA 1.6%	81.1 ± 2.8	29.26 ± 5.10	5.76 ± 0.31	–	–
AT 0.6%	84.0 ± 1.7	26.79 ± 4.20	0.95 ^a	–	–
AT 1.6%	82.5 ± 2.5	26.04 ± 4.20	0.58 ± 0.00	–	–

T_{out}: outlet air temperature.

^a Single determinations due to poor material quantity obtained.

^b (AA-AT)₇₅ 1.9% Different spray drying conditions were used.

Section 2.4 [64]. The pure AA powders had the highest moisture contents after spray drying due to the AA hygroscopic nature [59]. On the contrary, pure AT powder (non-hygroscopic material) had the lowest moisture content after processing.

3.3.2. Drug loading efficiency

The products (AA-AT)_x 1.3–8% present load efficiencies (Table 2) between 0.30 and 0.63 g_{AT}/g_{solid}. Considering that the bioavailability of AT administered by the inhalatory route should be better than that of the oral route, the new materials demonstrate to have dose flexibility and load efficiencies high enough to formulate AT inhalatory capsules.

It is important to remark that the relative composition of AT in the powder samples differs from the AT ratio in the dispersion (Tables 1 and 2). In fact, the AT/AA ratio in the powders is significantly higher than the relationship measured in the dispersion. This result is associated to a differential stickiness of AA to the chamber during spray-drying process, behaviour that will be further discussed in Section 3.3.4.

3.3.3. FT-IR characterization

For a molecular level characterization, FT-IR spectra of the spray-dried products (AA-AT)₂₅ 1.3%, (AA-AT)₅₀ 1.6% and (AA-AT)₇₅ 1.9%, AA 1%, AT 0.6%, raw pure materials (AT_{op} and AA_{op}) and the physical mixture (PM, with the same AA:AT proportion as the complex (AA-AT)₅₀ 1.6%) were characterized. To analyse if the spray drying leads to ionic complexes between AT and AA, Fig. 2 shows the FT-IR spectra for the samples above mentioned highlighting the following relevant bands:

- non-dissociated acidic or basic functional groups
- dissociated carboxylic and amino groups.

Raw and spray-dried pure AT and AA spectra showed the characteristic absorption bands of each substance previously reported in the literature [63,67]. This result indicates that the spray-drying process does not, as expected, degrade these compounds. Accordingly, only the spectra of the powders obtained by processing AT 0.6% and AA 1% were included in Fig. 2.

For the AT 0.6% powder, the bands ascribed to stretching and in-plane deformation of the N–H group were at 3160 cm⁻¹ and 1637 cm⁻¹, respectively in agreement with previous reports [68]. According to Soares et al. [63], the C=O stretching band of the AA is expected to be found around 1730 cm⁻¹. In consistency with the published data, Fig. 2 indicates that for the AA 1% sample the band ascribed to non-dissociated carboxylic groups showed up at 1755 cm⁻¹. As expected, the PM spectrum clearly showed the N–H bands of AT at 3164 and 1638 cm⁻¹ and the COOH band of AA at 1744 cm⁻¹.

The FT-IR spectra of binary spray-dried products showed some remarkable differences when they were compared to the above mentioned spectra (also depicted in Fig. 2).

The N–H bands, previously identified in the pure spray-dried AT sample, completely disappeared in the binary products spectra and a new band ascribed to NH₂⁺ wagging appeared at ~1600 cm⁻¹ (1594 cm⁻¹ for (AA-AT)₂₅ 1.3%, 1600 cm⁻¹ for (AA-AT)₅₀ 1.6% and 1609 cm⁻¹ for (AA-AT)₇₅ 1.9%). These changes suggested that the AT was completely consumed to produce the ionic complex.

Moreover, an intense band ascribed to the C=O asymmetric stretching of the carboxylate groups of AA was present at 1660 cm⁻¹ for (AA-AT)₂₅ 1.3%, at 1669 cm⁻¹ for (AA-AT)₅₀ 1.6% and at 1675 cm⁻¹ for (AA-AT)₇₅ 1.9% [69]. In addition, a band that correspond to the C=O symmetric stretching of the COO⁻ group appeared as a shoulder at 1400 cm⁻¹ for (AA-AT)₂₅ 1.3%, at 1413 cm⁻¹ for (AA-AT)₅₀ 1.6%

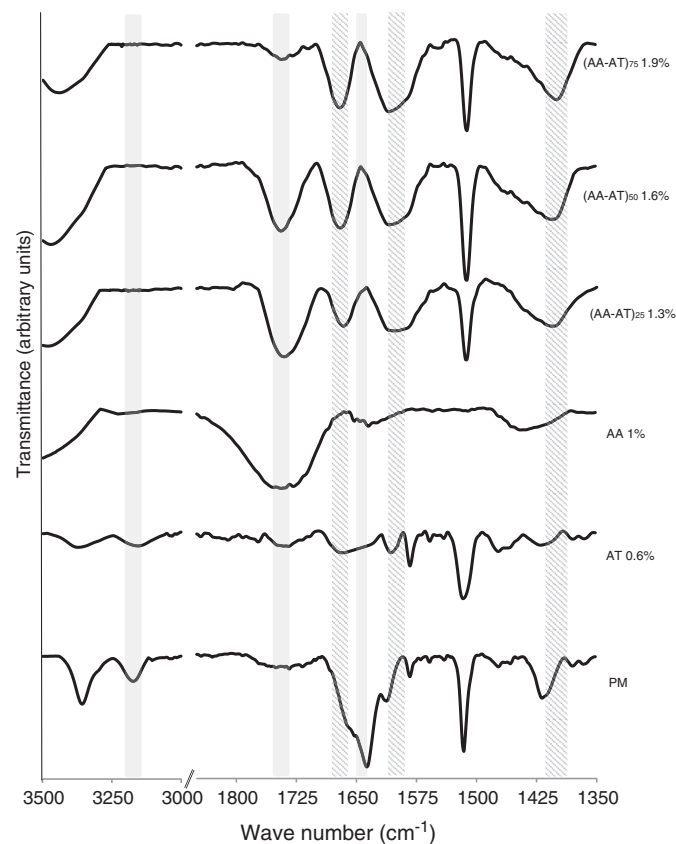


Fig. 2. FT-IR spectra of spray-dried pure materials, physical mixture (PM) of AA and AT and spray-dried (AA-AT)_x 1.3–1.9% complexes. Relevant bands are highlighted (solid fill, non-dissociated acidic or basic groups; dashed fill, dissociated carboxylic and amino groups).

and at 1402 cm^{-1} for $(\text{AA-AT})_{75}$ 1.9% [69]. The C=O stretching band of COOH of AA was still present in the binary spray-dried sample spectra at 1739 cm^{-1} for $(\text{AA-AT})_{25}$ 1.3%, 1740 cm^{-1} for $(\text{AA-AT})_{50}$ 1.6% and at 1739 cm^{-1} for $(\text{AA-AT})_{75}$ 1.9%. However the intensity of this band significantly decreased as the degree of neutralization increased.

The significant changes observed in $(\text{AA-AT})_x$ 1.3–1.9% materials with regard to pure materials and PM prove the ionic interaction between AT amino groups and the carboxylic groups of AA. These substances co-processed by spray drying resulted in a new chemical entity in the solid state, which is referred as polyelectrolyte–drug complex.

3.3.4. Thermal analysis

Thermal behaviour of the samples previously analysed by FT-IR (Section 3.3.3) was studied by DSC and the relevant results are presented in Table 3. The thermograms of AT (raw and spray-dried materials) presented an endothermic event at $153.48\text{ }^\circ\text{C}$, associated to the drug melting [41]. This peak was also identified in the PM at $153.83\text{ }^\circ\text{C}$, however it was not detected for the $(\text{AA-AT})_x$ 1.3–1.9% samples (see Table 3). Thermal properties of a physical mixture are equivalent to the sum of individual components thermograms [70] and deviation from this behaviour indicates some kind of interaction between components [71]. In binary spray-dried powders, the lack of the melting endotherm was an indirect evidence that the crystalline structure of AT was absent. This fact together with FT-IR analysis ensures the ionic interaction between AA and the drug.

DSC thermograms of AA_{op} , AA 1% and $(\text{AA-AT})_x$ 1.3–1.9% materials further showed a broad endotherm at temperature nearly $100\text{ }^\circ\text{C}$ [63] which was associated to the loose of sorpted water (this endotherm was only present during the first heating of the sample).

Once water was eliminated, glass transition temperature (T_g) of AA and complexes samples can be determined during the second heating. Table 3 also shows the T_g values of the pure AA and the $(\text{AA-AT})_x$ 1.3–1.9% powders. The T_g value increased as the neutralization degree was raised. This behaviour could be attributed to an anti-plasticizer effect of AT in AA structure. It is postulated that this drug was localized in the free volume between the chains of the polymers linked with them by electrostatic interaction [72]. The same effect on T_g was reported for other systems where the polyelectrolyte was associated with smaller molecules through strong interactions, such as ionic ones [73].

The T_g values can also be related to stickiness of the materials during spray drying [74–78]. In this sense, Bhandari et al. [76] proposed that inlet air temperature should not be higher than $20\text{ }^\circ\text{C}$ above the T_g of the material that is dried in order to improve the process yield. In the spray drying of the binary samples no yield problems were observed because of the outlet air temperatures were lower than the T_g values (see Table 2). However, considering that: a) there was remaining free AA (nonassociated to AT) in all the binary feed formulations, and b) in some area of the drying chamber, the temperature could be close to the AA T_g ($110\text{ }^\circ\text{C}$), selective stickiness of AA on the spray-dryer chamber could be expected. In fact, different AT compositions in

the binary dispersions (Table 1) and the binary powder (Table 2) were found.

3.3.5. Crystallographic characterization

Crystallographic analysis of samples (previously mentioned in Section 3.3.3.) was addressed with the aim to identify crystalline changes associated to process and composition of atomized dispersions. According to the AT_{op} diffractogram, the pure sample had crystalline structure. The position and intensity of the reflections (Fig. 3) were in agreement with data reported by Ficarra et al. [71]. The 100-relative intensity peak was found at the inter-planar spacing of 12.4 ° , in concordance with the reported values [79]. For the AT powder obtained from the AT 0.6% dispersion, this peak became less intense as it is depicted in Fig. 3. This sample maintained the crystalline structure (the reflections were in the same angular positions than the ones of AT_{op}), however the crystallinity degree [80] and crystal habit were different as consequence of the process that it was subjected to [68].

The Scherrer equation was used to compare the crystallinity degree of unprocessed and spray-dried samples [47]. For the AT_{op} , the crystalline packet size responsible for the peak at 12.4 ° was 149 nm and for AT 0.6% was 42 nm , proving that the spray drying modifies the crystallinity degree. In addition, the crystallinity loss could be also confirmed by the elevation of the baseline from 15 to 30 ° , characteristic behaviour of amorphous materials.

Regarding the acid polyelectrolyte, AA_{op} presented a structure formed by crystalline regions with peaks at 15.1 and 20.0 ° (characteristic peaks founded by Ikeda et al. [80]). Also, due to the baseline elevation from 15 to 40 ° , it can be concluded that the crystalline structure was immersed in an amorphous matrix [80]. The powder obtained by spray drying of the AA 1% dispersion showed an arrangement even more disordered than AA_{op} (see peak at 15.1 ° , Fig. 3).

The PM diffractogram showed the characteristics reflections of both materials: AA_{op} and AT_{op} (see Fig. 3).

Interestingly, the spray-dried binary products presented diffraction patterns of amorphous substances as it was expected from the DSC thermograms previously discussed in Section 3.3.4. The reflections associated with AT crystalline structure were absent and those related with AA crystalline portions were substantially modified, particularly when the neutralization degree was increased to 75% (Fig. 3).

These results indicated that fast drying of AT is not enough to explain the amorphous structure of the drug in the binary product. The interaction between the macromolecule and the drug prevents AT crystallization during the process studied.

3.3.6. Morphology

Depending on the feed formulation and operating conditions, the spray-drying technique allows producing particulate systems of varied shapes [81]. For this reason, the sample morphology was studied by scanning electronic microscopy (SEM). Fig. 4 shows micrographs of spray-dried and unprocessed samples of the pure compounds. The

Table 3

Thermal behaviour of pure materials, $(\text{AA-AT})_x$ 1.3–1.9% spray-dried powders and the physical mixture of AA and AT (PM).

Sample	Vitreous transition (T_g) ($^\circ\text{C}$)	ΔC_p ($\text{J/g } ^\circ\text{C}$)	Melting (T_{onset}) ($^\circ\text{C}$) ^a	ΔH_m (J/g) ^a
$(\text{AA-AT})_{25}$ 1.3%	111.01 ± 0.39	0.21 ± 0.02	Not present	–
$(\text{AA-AT})_{50}$ 1.6%	125.67 ± 1.02	0.21 ± 0.01	Not present	–
$(\text{AA-AT})_{75}$ 1.9%	133.32 ± 0.53	0.43 ± 0.04	Not present	–
AA_{op}	110.65 ± 2.47	0.44 ± 0.06	–	–
AA 1%	110.97 ± 3.18	0.21 ± 0.04	–	–
AT_{op}	–	–	153.48	128.22
AT 0.6%	–	–	152.62	103.30
PM	109.98 ± 2.95	0.22 ± 0.05	153.83	45.45

^a Single determinations.

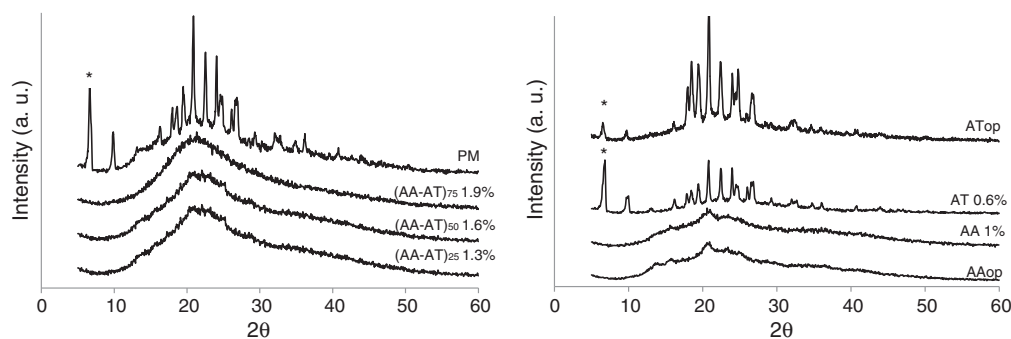


Fig. 3. Sample diffractograms (a. u.: arbitrary units): left, (AA-AT)_x complexes and physical mixture (PM) of AA_{op} and AT_{op}; right, raw and spray-dried pure materials.

AA_{op} particles were irregular with rough and porous surfaces (Fig. 4I), while the AT_{op} powder exhibited irregularly shaped platelets of different sizes joined in clusters (Fig. 4IV). The observed morphology for the AT_{op} sample was in good agreement with the one reported by Marini, et al. [79]. As it is shown in Fig. 4II & III, the powder obtained from AA 1% was constituted mainly by buckled particles, however fibre-type particles bigger than the buckled ones were also observed. The spray-dried AT 0.6% dispersion (Fig. 4V & VI) led to polyhedral shape particles; plane faces of particles could be associated to the crystalline nature of this solid after drying. The spray-dried pure materials showed smooth surfaces (Fig. 4III & VI).

Fig. 5 shows spray-dried binary materials obtained from dispersions with equal neutralization degree and different solid contents. For all the powders, crumpled particles with wrinkle surfaces were observed. These morphologies were expected for polymeric-based particles [82] and were different from the spray-dried pure materials. No crystals were observed as expected from DSC and PXRD experiments reinforcing the idea that AT was completely associated to the AA.

For polymeric materials it was proposed that there was not uniform distribution of the material in the droplet during drying. The low

diffusion of the macromolecule causes material enrichment in the droplet surface and a shell was formed in earlier stages of the process. Depending on the shell attributes (thickness and mechanical properties), it may collapse or wrinkle resulting in products with buckled or crumpled shapes [81]. Based on this theory, the differentiated shapes between AA-AT products and pure AA 1% could indicate that the interaction between AT and AA significantly change the shell properties. In addition, it was observed that the depressions of the binary particles were attenuated as the solid content increased probably because of a shell more resistant to deformation was formed during the process.

3.3.7. Flow properties of powders

Table 4 shows the bulk and tap densities, Carr index and repose angle found for the different AA-AT formulations. According to the USP powder classification based on the Carr index (given in Section 2.5.5), the complexes presented “very poor” or “very, very poor” flow properties [40]. On the other hand, the angle of repose data indicated that the products have “regular” or “poor” flow properties (Section 2.5.5). The apparent lack of correlation between both determinations was explained by the presence of unstable agglomerates in the particulate formulations [83].

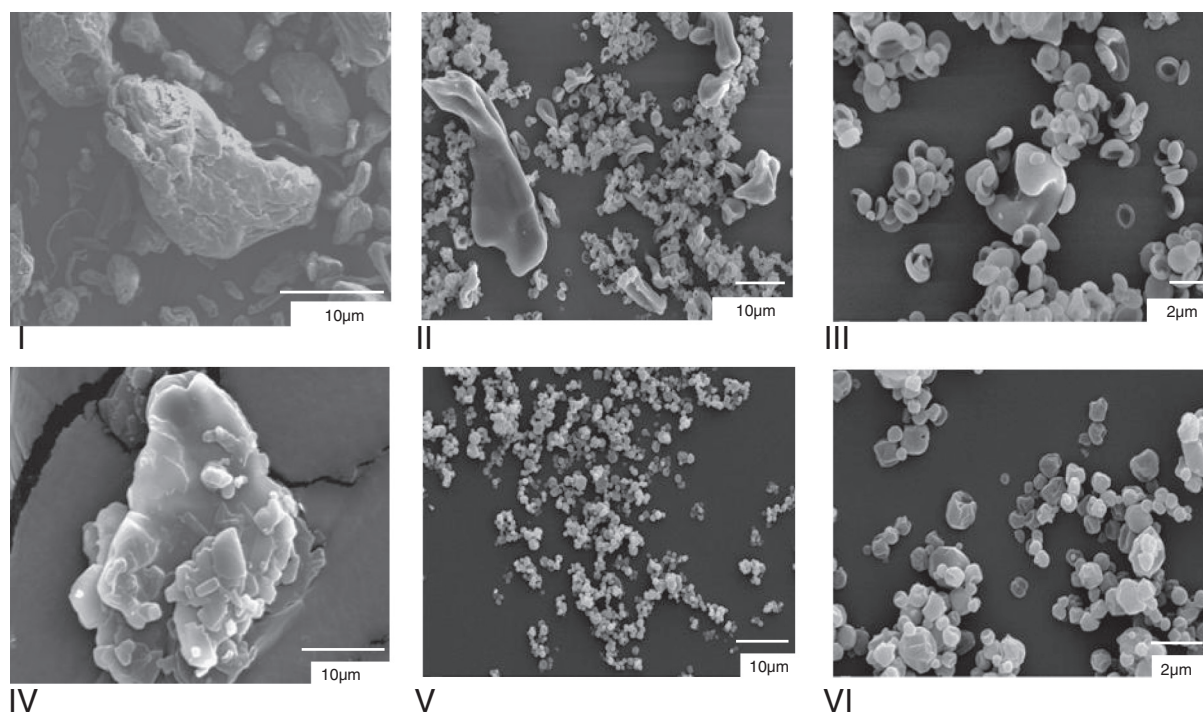


Fig. 4. SEM photographs of pure materials: I) AA_{op} (3000×), II) AA 1% (3000×), III) AA 1% (10000×), IV) AT_{op} (3000×), V) AT 0.6% (3000×) and VI) AT 0.6% (10000×).

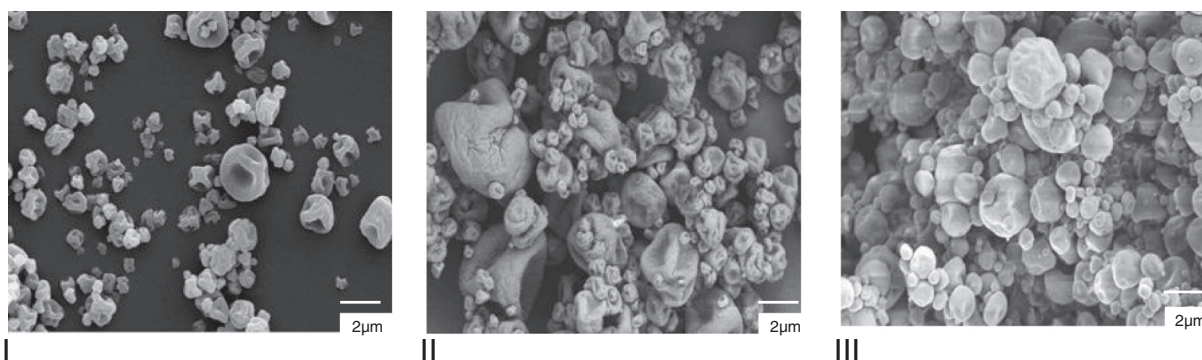


Fig. 5. SEM photographs of the products: I) (AA-AT)₅₀ 1.6%, II) (AA-AT)₅₀ 4% and III) (AA-AT)₅₀ 8% (8000× of magnification).

These aggregates improved the powder flow properties and led to repose angles representative of regular or poor flows. However, the unstable agglomerates were easily disaggregated into individual particles when samples were tapped during tap density measurements (data used in Carr index calculation). This powder behaviour led to high Carr indexes which, in contrast to the repose angle measurements, indicated bad flow properties.

These results are in agreement with the low particle size (see Section 3.3.9) of the obtained materials. Respirable microparticles are considered cohesive powders that often exhibit problems to flow and agglomeration predisposition [84], mainly because the bed behaviour of fine powders (<30 μm) is controlled by interparticle interactions (predominantly Van der Waals attractive forces) [83]. However, the flowability and agglomeration tendency can be significantly improved with the addition of excipients (carriers), like lactose [18,85].

3.3.8. Hygroscopicity

As above discussed, the AA has a high hygroscopicity [59]. For this reason, the conditioned raw AA powder presented a final moisture content of 75% w/w (Table 4), value that was one order of magnitude higher than the initial one (7.24% w/w, see Table 2). On the other hand, the powders obtained from (AA-AT)_x 1.3–8% dispersions increased the moisture content from 3.43–5.32 (Table 2) to 16.50–24.18% w/w (Table 4). This marked decrease of final hygroscopicities of the binary products compared to that of pure AA is desired in order to avoid stability problems during handling and storage of these powders.

3.3.9. Particle size distribution, powder density and aerodynamic diameter

Complexes presented volumetric mean diameters between 5.50 and 6.97 μm (Table 5). For the same neutralization degree, when the solid content was augmented from 1.6 to 4% the mean particle diameter increased in about 15% probably associated to earlier shell consolidation [81]. Further solid content increases did not affect the mean diameter. The formulations allowed producing narrow particle size distributions, being the span lower than 2 for all of them.

The spray-dried powder skeletal densities were between 0.90 and 1.38 g/cm³ (Table 5). Considering that AT_{op} and AA_{op} have solid densities

of 1.13 and 1.60 g/cm³ [86,87], respectively, it can be inferred that the particles could be hollow [81]. For the same AT/AA ratio, higher densities were found for samples obtained from more concentrated feed solutions. This behaviour is in good agreement with the results reported by Vehring [81].

Since the powders obtained from (AA-AT)₅₀ 4 and 8% had almost the same volumetric diameter, the density values indicate that the (AA-AT)₅₀ 4% powder could be constituted by hollower particles than the ones of (AA-AT)₅₀ 8%.

Table 5 also shows the mean D_{aer} calculated according to Eq. (5). The lowest D_{aer} was found for the powder (AA-AT)₇₅ 1.9%. VanOort [88] establishes 10 μm as the maximum D_{aer} for inhalatory administration, therefore (AA-AT)₇₅ 1.9% formulation appeared to be the best one from a size point of view. This sample had also good attributes such as: highest load efficiency, low residual moisture and good process yield. Nevertheless, the D_{aer} distribution has to be evaluated in order to know the mass percentage that can reach the pulmonary membrane.

Fig. 6 shows the D_{aer} distribution (calculated from the mass size distribution affected by the square root of the skeletal density) for (AA-AT)₇₅ 1.9% formulation. The 89.0% of the powder had aerodynamic diameters lower than 10 μm. Even if this formulation had good properties for the selected application, with the aim to maximize the respirable fraction, the (AA-AT)₇₅ 1.9% dispersion was atomized increasing the atomization air volumetric flow rate from 601 L/h to 742 L/h, ((AA-AT)₇₅ 1.9%^b). Consequently, as it is also shown in Fig. 6, the cumulative fraction of particles lower than 10 μm increased from 89.0% to 94.4% (Fig. 6). This improvement in size quality caused simultaneously a decrease in the yield of 67.4 to 45.8% (Table 2), problem that can be overcome by using a high efficiency cyclone. Therefore, there is still flexibility to further improve the powders by optimizing the spray-drying operating conditions and the collection device.

4. Conclusions

By using an anionic polyelectrolyte (AA), a novel powder to deliver AT by the inhalatory route was developed. The ionic interaction between both components was proved, so a new chemical entity was

Table 4
Hygroscopicity and flow properties (AA-AT)_x 1.3–8% spray-dried powders.

Sample	Hygroscopicity (%)	D _{bulk} (g/cm ³)	D _{tap} (g/cm ³)	Carr index (%)	Angle of repose (°)
(AA-AT) ₂₅ 1.3%	16.50 ± 0.57	0.27 ± 0.01	0.44 ± 0.01	36.98 ± 4.30	31.84 ± 2.71
(AA-AT) ₅₀ 1.6%	19.16 ± 0.86	0.28 ± 0.03	0.43 ± 0.02	36.02 ± 3.48	31.87 ± 3.80
(AA-AT) ₇₅ 1.9%	21.53 ± 0.64	0.26 ± 0.01	0.44 ± 0.01	40.64 ± 0.62	31.78 ± 3.41
(AA-AT) ₅₀ 4%	20.07 ± 0.47	0.27 ± 0.01	0.47 ± 0.02	41.66 ± 3.06	31.47 ± 5.92
(AA-AT) ₅₀ 8%	24.18 ± 0.64	0.25 ± 0.01	0.43 ± 0.03	43.26 ± 4.87	31.47 ± 5.86
AA _{op}	75.29 ± 0.41 ^a	–	–	–	–

D_{bulk}: bulk density, D_{tap}: tap density.

^a Hygroscopicity value determined as a reference.

Table 5
Mean diameter, span, solid density and aerodynamic diameter of products and pure materials.

Sample	D ₄₃ (μm)	Span	D _s (g/cm^3)	Median D _{aer} (μm)
(AA–AT) ₂₅ 1.3%	5.59 \pm 0.08	1.02	1.38 \pm 0.02	6.56
(AA–AT) ₅₀ 1.6%	5.50 \pm 0.30	1.26	1.01 \pm 0.04	5.52
(AA–AT) ₇₅ 1.9%	5.64 \pm 0.05	1.08	0.90 \pm 0.06	5.29
(AA–AT) ₅₀ 4%	6.33 \pm 0.36	1.02	1.08 \pm 0.05	6.57
(AA–AT) ₅₀ 8%	6.31 \pm 0.24	1.04	1.26 \pm 0.03	6.98
(AA–AT) ₂₅ 1.6%	6.37 \pm 0.32	0.93	1.16 \pm 0.03	7.18
(AA–AT) ₇₅ 1.6%	6.97 \pm 0.08	0.97	1.13 \pm 0.05	8.87
(AA–AT) ₇₅ 1.9% ^b	5.15 \pm 0.11	1.11	0.93 \pm 0.06	4.97
AA _{op}	53.44 \pm 0.98	1.94	1.60 [87]	–
AA 1%	8.95 \pm 0.26	1.43	–	–
AA 1.6%	7.68 \pm 0.07	2.13	–	–
AT _{op}	61.25 \pm 0.71	1.98	1.10 [86]	–
AT 0.6%	6.07 \pm 0.36	1.16	–	–
AT 1.6%	8.50 \pm 0.93	2.15	–	–

D₄₃: mean volumetric diameter, D_s: skeletal density, D_{aer}: aerodynamic diameter.

[87] A. Rachocki et al. (2011).

[86] S. Budavari (2007).

formed by an aqueous-based spray drying process. It is expected that this material could improve the drug targeting to the respiratory membrane and increase its time residence because of the mucoadhesive properties of the polymeric chains. The proposed new materials exhibit flexibility to load different drug contents. Feed solid content and viscosity were the main variables that modify the process yield and product quality. The formulations with the best attributes for inhalatory applications showed low moisture content, high load efficiency, low mean aerodynamic diameters and high respirable fraction. Even though, the new materials fulfil the requirements for inhalatory products, they can be optimized, for example, by changing the spray-drying operating conditions. In vitro deposition and dissolution, in vitro/ex vivo membrane permeation and in vivo evaluation are some of the further studies that have to be carry out for a complete characterization of the proposed formulations.

Acknowledgements

FONCyT (PICT-PRH 2009-0124), CONICET (PIP 112-2011-0100336 112) and UNS (PGI 24/B209) grants support this study. N.E.C. thanks CONICET for her doctoral fellowship. The authors thank Lic. F. Cabrera (PLAPIQUI) for her technical assistance.

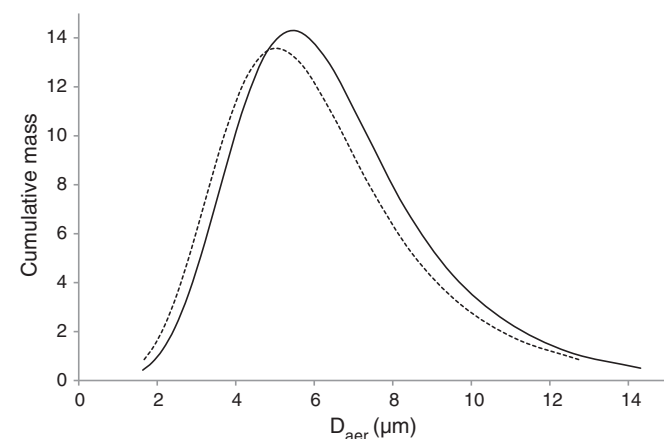


Fig. 6. Estimated D_{aer} for (AA–AT)₇₅ 1.9% (complete line) and (AA–AT)₇₅ 1.9%^b (dashed line).

References

- [1] D.I. Daniher, J. Zhu, Dry powder platform for pulmonary drug delivery, *Particuology* 6 (2008) 225–238.
- [2] T.C. Carvalho, J.J. Peters, R.O. Williams, Influence of particle size on regional lung deposition—what evidence is there? *Int. J. Pharm.* 406 (2011) 1–10.
- [3] F. Buttini, P. Colombo, A. Rossi, F. Sonvico, G. Colombo, Particles and powders: tools of innovation for non-invasive drug administration, *J. Control. Release* 161 (2012) 693–702.
- [4] Pulmonary drug delivery, in: N. Washington, C. Washington, C. Wilson (Eds.), *Physiological Pharmaceutics. Barriers to Drug Absorption*, Taylor & Francis, 2001, pp. 221–247.
- [5] L. Gallo, J.M. Llabot, D. Allemandi, V. Bucalá, J. Piña, Influence of spray-drying operating conditions on *Rhannus purshiana* (Cáscara sagrada) extract powder physical properties, *Powder Technol.* 208 (2011) 205–214.
- [6] A. Chow, H. Tong, P. Chattopadhyay, B. Shekunov, Particle engineering for pulmonary drug delivery, *Pharm. Res.* 24 (2007) 411–437.
- [7] A.B.D. Nandiyanto, K. Okuyama, Progress in developing spray-drying methods for the production of controlled morphology particles: from the nanometer to submicrometer size ranges, *Adv. Powder Technol.* 22 (2011) 1–19.
- [8] M. Beck-Broichsitter, C. Schweiger, T. Schmehl, T. Gessler, W. Seeger, T. Kissel, Characterization of novel spray-dried polymeric particles for controlled pulmonary drug delivery, *J. Control. Release* 158 (2012) 329–335.
- [9] W.S. Cheow, K. Hadinoto, Green preparation of antibiotic nanoparticle complex as potential anti-biofilm therapeutics via self-assembly amphiphile–polyelectrolyte complexation with dextran sulfate, *Colloids Surf. B: Biointerfaces* 92 (2012) 55–63.
- [10] W.S. Cheow, K. Hadinoto, Self-assembled amorphous drug–polyelectrolyte nanoparticle complex with enhanced dissolution rate and saturation solubility, *J. Colloid Interface Sci.* 367 (2012) 518–526.
- [11] M. Hess, R.G. Jones, J. Kahovec, T. Kitayama, P. Kratochvíl, P. Kubisa, et al., Terminology of polymers containing ionizable or ionic groups and of polymers containing ions (IUPAC Recommendations 2006), *Pure Appl. Chem.* 78 (2006) 2067–2074.
- [12] H.M. Mansour, M. Sohn, A. Al-Ghananeem, P.P. Deluca, Materials for pharmaceutical dosage forms: molecular pharmaceuticals and controlled release drug delivery aspects, *Int. J. Mol. Sci.* 11 (2010) 3298–3322.
- [13] C. Colonna, B. Conti, I. Genta, O.H. Alpar, Non-viral dried powders for respiratory gene delivery prepared by cationic and chitosan loaded liposomes, *Int. J. Pharm.* 364 (2008) 108–118.
- [14] P. Opanasopit, T. Rojanarata, A. Apirakaramwong, T. Ngawhirunpat, U. Ruktanonchai, Nuclear localization signal peptides enhance transfection efficiency of chitosan/DNA complexes, *Int. J. Pharm.* 382 (2009) 291–295.
- [15] K.T. Al-Jamal, W.T. Al-Jamal, J.T.-W. Wang, N. Rubio, J. Buddle, D. Gathercole, et al., Cationic poly-L-lysine dendrimer complexes doxorubicin and delays tumor growth in vitro and in vivo, *ACS Nano* 7 (2013) 1905–1917.
- [16] N. Mohajel, R. Najafabadi, K. Azadmanesh, A. Vatanara, E. Moazeni, A. Rahimi, et al., Optimization of a spray drying process to prepare dry powder microparticles containing plasmid nanocomplex, *Int. J. Pharm.* 423 (2012) 577–585.
- [17] F. Gong, H. Tang, Y. Lin, W. Gu, W. Wang, M. Kang, Gene transfer of vascular endothelial growth factor reduces bleomycin-induced pulmonary hypertension in immature rabbits, *Pediatr. Int.* 47 (2005) 242–247.
- [18] K. Kho, K. Hadinoto, Dry powder inhaler delivery of amorphous drug nanoparticles: effects of the lactose carrier particle shape and size, *Powder Technol.* 233 (2013) 303–311.
- [19] H. Swai, K.T. Hillie, N. Cingo, L. Kalombo, M. Legodi, B. Semete, Evaluation of nano encapsulation techniques in different polymeric system for the delivery of anti-tuberculosis drugs (ATD), CSRI, 2003. 1.

- [20] N. Sivasdas, D.O. Rourke, A. Tobin, V. Buckley, Z. Ramtoola, J.G. Kelly, et al., A comparative study of a range of polymeric microspheres as potential carriers for the inhalation of proteins, *Int. J. Pharm.* 358 (2008) 159–167.
- [21] R.O. Williams, M.K. Barron, M. Jose, C. Remun, Investigation of a pMDI system containing chitosan microspheres and P134a, *Int. J. Pharm.* 174 (1998) 209–222.
- [22] S. Chand, A. Singh, A. Kumar, A. Mishra, Review on production and medical applications of -polylysine, *Biochem. Eng. J.* 65 (2012) 70–81.
- [23] H.M. Mansour, Y.-S. Rhee, X. Wu, Nanomedicine in pulmonary delivery, *Int. J. Nanomedicine* 4 (2009) 299–319.
- [24] Y. Yang, W.S. Cheow, K. Hadinoto, Dry powder inhaler formulation of lipid-polymer hybrid nanoparticles via electrostatically-driven nanoparticle assembly onto microscale carrier particles, *Int. J. Pharm.* 434 (2012) 49–58.
- [25] R. Krishnamoorthy, A.K. Mitra, Prodrugs for nasal drug delivery, *Adv. Drug Deliv. Rev.* 29 (1998) 135–146.
- [26] S. Salpeter, T. Ormiston, E. Salpeter, P. Poole, C. Cates, Cardioselective beta-blockers for chronic obstructive pulmonary disease: a meta-analysis, *Respir. Med.* 97 (2003) 1094–1101.
- [27] J.A. García-Sevilla, F. Barturen, Fármacos que modifican la actividad simpática, in: Jesús Florez, Juan Antonio Armiño y África Mediavilla (Eds.), *Farmacología Humanafourth ed.*, 1997, pp. 261–275.
- [28] N. Dew, T. Bramer, K. Edsman, Catanionic aggregates formed from drugs and lauric or capric acids enable prolonged release from gels, *J. Colloid Interface Sci.* 323 (2008) 386–394.
- [29] T.C. Westfall, D.D. Westfall, Agonistas y antagonistas adrenérgicos, in: Goodman, Gilman (Eds.), *Las bases farmacológicas de la terapéutica*, eleventh ed., McGrawHill, 1998, pp. 237–295.
- [30] Y. F. Maa, S. J. Prestertski, T. L. Burkoth, Spray freeze-dried compositions, United States Patent, 0202978-A1 (2003).
- [31] A. Tronde, Pulmonary drug absorption, in vitro and in vivo investigations of drug absorption across the lung and its relation to drug physicochemical properties, 2002. (PhD Thesis).
- [32] N.M. Hawkins, M.C. Petrie, M.R. Macdonald, P.S. Jhund, L.M. Fabbri, J. Wikstrand, et al., Heart failure and chronic obstructive pulmonary disease the quandary of beta-blockers and beta-agonists, *J. Am. Coll. Cardiol.* 57 (2011) 2127–2138.
- [33] J. D. Rabinowitz, A. C. Zaffaroni, Delivery of beta-blockers through an inhalation route. PCT WO 02/094237-A1, (2002).
- [34] A.F. Jimenez-Kairuz, J.M. Llabot, D.A. Allemandi, R.H. Manzo, Swellable drug-polyelectrolyte matrices (SDPM). Characterization and delivery properties, *Int. J. Pharm.* 288 (2005) 87–99.
- [35] M.V. Ramirez Rigo, D.A. Allemandi, R.H. Manzo, Swellable drug-polyelectrolyte matrices (SDPM) of alginate acid characterization and delivery properties, *Int. J. Pharm.* 322 (2006) 36–44.
- [36] A. Zahoor, S. Sharma, G.K. Khuller, Inhalable alginate nanoparticles as antitubercular drug carriers against experimental tuberculosis, *Int. J. Antimicrob. Agents* 26 (2005) 298–303.
- [37] S. Tiwari, A.P. Chaturvedi, Y.B. Tripathi, B. Mishra, Microspheres based on mannosylated lysine-co-sodium alginate for macrophage-specific delivery of isoniazid, *Carbohydr. Polym.* 87 (2012) 1575–1582.
- [38] K. Möbus, J. Siepmann, R. Bodmeier, Zinc-alginate microparticles for controlled pulmonary delivery of proteins prepared by spray-drying, *Eur. J. Pharm. Biopharm.* 81 (2012) 121–130.
- [39] V. Delgado, F. González-Caballero, R.J. Hunter, L.K. Koopal, J. Lyklema, Measurement and interpretation of electrokinetic phenomena, *J. Colloid Interface Sci.* 309 (2007) 194–224.
- [40] United States Pharmacopeia, National Formulary, The United States Pharmacopeial Convention, USP 30-NF 25, 2007. (Rockville, MD.).
- [41] V. Caplar, Z. Mikotic-Mihum, H. Hofman, J. Kuftinec, F. Kajfez, A. Nagl, N. Blazevic, Atenolol, in: Florey (Ed.), *Analytical Profiles of Drugs Substances*, thirteenth ed., Academic Press Inc., 1984, pp. 2–25.
- [42] A. Schoubben, P. Blasi, S. Giovagnoli, C. Rossi, M. Ricci, Development of a scalable procedure for fine calcium alginate particle preparation, *Chem. Eng. J.* 160 (2010) 363–369.
- [43] K. Mladenovska, O. Cruaud, P. Richomme, E. Belamie, R.S. Raicki, M. Venier-Julienne, et al., 5-ASA loaded chitosan-Ca-alginate microparticles: preparation and physicochemical characterization, *Int. J. Pharm.* 345 (2007) 59–69.
- [44] S. Shoyele, N. Sivasdas, S. Cryan, The effects of excipients and particle engineering on the biophysical stability and aerosol performance of parathyroid hormone (1–34) prepared as a dry powder for inhalation, *AAPS PharmSciTech* 12 (2011) 304–311.
- [45] C. Muzzarelli, V. Stanic, L. Gobbi, G. Tosi, R. Muzzarelli, Spray-drying of solutions containing chitosan together with polyuronans and characterisation of the microspheres, *Carbohydr. Polym.* 57 (2004) 73–82.
- [46] J.D. Ormes, D. Zhang, A.M. Chen, S. Hou, D. Krueger, T. Nelson, et al., Design of experiments utilization to map the processing capabilities of a micro-spray dryer: particle design and throughput optimization in support of drug discovery, *Pharm. Dev. Technol.* (2012) 1–9.
- [47] A.W. Burton, K. Ong, T. Rea, I.Y. Chan, On the estimation of average crystallite size of zeolites from the Scherrer equation: a critical evaluation of its application to zeolites with one-dimensional pore systems, *Microporous Mesoporous Mater.* 117 (2009) 75–90.
- [48] M.L. Ramón García, Determinación del tamaño de cristal utilizando el software Jade 6.5, Universidad Nacional Autónoma, México, 2007. 1–52.
- [49] F. Palazzo, S. Giovagnoli, A. Schoubben, P. Blasi, C. Rossi, M. Ricci, Development of a spray-drying method for the formulation of respirable microparticles containing ofloxacin-palladium complex, *Int. J. Pharm.* 440 (2013) 273–282.
- [50] W. Kaialy, A. Alhalaweh, S.P. Velaga, A. Nokhodchi, Effect of carrier particle shape on dry powder inhaler performance, *Int. J. Pharm.* 421 (2011) 12–23.
- [51] J.L. Vila Jato, Formas Farmacéuticas Orales, in: Vila Jato (Ed.), *Tecnología Farmacéutica*, third ed., Formas farmacéuticas, Síntesis, vol II, 2001, pp. 56–156.
- [52] Standard Practice for Maintaining Constant Relative Humidity by Means of Aqueous Glycerin Solutions, in: ASTM International (Ed.), *Norm D5032-97*, 2003.
- [53] H.C. Wang, W. John, Particle density correction for the aerodynamic particle sizer, *Aerosol Sci. Technol.* 6 (1987) 191–198.
- [54] G.S. Manning, Limiting laws and counterion condensation in polyelectrolyte solutions I. Colligative properties, *J. Chem. Phys.* 51 (1969) 924.
- [55] G.S. Manning, Limiting laws and counterion condensation in polyelectrolyte solutions II. Self-diffusion of the small ions, *J. Chem. Phys.* 51 (1969) 934.
- [56] A.F. Jimenez-Kairuz, D.A. Allemandi, R.H. Manzo, Equilibrium properties and mechanism of kinetic release of metoclopramide from carbomer hydrogels, *Int. J. Pharm.* 250 (2003) 129–136.
- [57] F.D. Battistini, M.E. Olivera, R.H. Manzo, Equilibrium and release properties of hyaluronic acid-drug complexes, *Eur. J. Pharm. Sci.* 49 (2013) 588–594.
- [58] M.V. Ramírez Rigo, D.A. Allemandi, R.H. Manzo, A linear free energy relationship treatment of the affinity between carboxymethylcellulose and basic drugs, *Mol. Pharm.* 1 (2004) 383–386.
- [59] R. Rowe, P. Sheskey, M. Quinn, Alginate acid, *Handbook of Pharmaceutical Excipients*, sixth ed., Pharmaceutical Press, 2009. 20–22.
- [60] M.G. Carneiro-da-Cunha, M. Cerqueira, B.W.S. Souza, J. Teixeira, A. Vicente, Influence of concentration, ionic strength and pH on zeta potential and mean hydrodynamic diameter of edible polysaccharide solutions envisaged for multilayered films production, *Carbohydr. Polym.* 85 (2011) 522–528.
- [61] R.P. Raffin, D.S. Jornada, I. Ré, A. Pohlmann, S.S. Guterres, Sodium pantoprazole-loaded enteric microparticles prepared by spray drying: effect of the scale of production and process validation, *Int. J. Pharm.* 324 (2006) 10–18.
- [62] M. Wesolowski, B. Rojek, Thermogravimetric detection of incompatibilities between atenolol and excipients using multivariate techniques, *J. Therm. Anal. Calorim.* 43 (2013) 169–177.
- [63] J.P. Soares, J.E. Santos, G.O. Chierice, E.T.G. Cavalheiro, Thermal behavior of alginate acid and its sodium salt, *Eclét. Quím.* 29 (2004) 57–64.
- [64] M.I.U. Islam, T.G. Langrish, An investigation into lactose crystallization under high temperature conditions during spray drying, *Food Res. Int.* 43 (2010) 46–56.
- [65] S.J. Lukasiewicz, Spray-drying ceramic powders, *J. Am. Ceram. Soc.* 24 (1989) 617–624.
- [66] N.R. Rabbani, P.C. Seville, The influence of formulation components on the aerosolisation properties of spray-dried powders, *J. Control. Release* 110 (2005) 130–140.
- [67] C. Ayala, R. Brunetto, F. Ovalles, Determination of atenolol in pharmaceutical dosages by Fourier transform infrared spectrometry (FTIR), *Univ. Zulia* 32 (2009) 238–248.
- [68] R. de Castro, R.M. Barbosa, J. Sim, Infrared spectroscopy of racemic and enantiomeric forms of atenolol, *Spectrochim. Acta A* 67 (2007) 1194–1200.
- [69] T.W. Wong, L.W. Chan, S.B. Kho, P.W. Sia Heng, Design of controlled-release solid dosage forms of alginate and chitosan using microwave, *J. Control. Release* 84 (2002) 99–114.
- [70] J. Wells, Pharmaceutical reformulation: the physicochemical properties of drug substances, in: M. Aulton (Ed.), *Pharmaceutics, The Science of Dosage Form Design*, second ed., Churchill Livingstone Elsevier Science Limited, 2002, pp. 113–138.
- [71] R. Ficarra, P. Ficarra, M.R.D. Bella, D. Raneri, S. Tommasini, M.L. Calabro, et al., Study of the inclusion complex of atenolol with β -cyclodextrins, *J. Pharm. Biomed. Anal.* 23 (2000) 231–236.
- [72] R.J. Chokshi, H.K. Sandhu, R.M. Iyer, N.H. Shah, W. Malick, H. Zia, Characterization of physico-mechanical properties of indomethacin and polymers to assess their suitability for hot-melt extrusion process as a means to manufacture solid dispersion/solution, *J. Pharm. Sci.* 94 (2005) 2463–2474.
- [73] A.L. Sarode, H. Sandhu, N. Shah, W. Malick, H. Zia, Hot melt extrusion (HME) for amorphous solid dispersions: predictive tools for processing and impact of drug-polymer interactions on supersaturation, *Eur. J. Pharm. Sci.* 48 (2012) 371–384.
- [74] B. Bhandari, T. Howes, Relating the stickiness property of foods undergoing drying and dried products to their surface energetics, *Dry. Technol.* 23 (2005) 37–41.
- [75] G.M. Miravet Valero, M. Alacid Cárceles, J.M. Obón de Castro, Secado por Atomización de zumo de granada, Universidad Politécnica De Cartagena, 2009. 1–152.
- [76] B. Bhandari, T. Howes, Implication of glass transition for the drying and stability of dried foods, *J. Food Eng.* 40 (1999) 71–79.
- [77] A.M. Goula, K.G. Adamopoulos, A new technique for spray drying orange juice concentrate, *Innovative Food Sci. Emerg. Technol.* 11 (2010) 342–351.
- [78] T.G. Langrish, Assessing the rate of solid-phase crystallization for lactose: the effect of the difference between material and glass-transition temperatures, *Food Res. Int.* 41 (2008) 630–636.
- [79] A. Marini, V. Berbenni, M. Pegoretti, G. Bruni, P. Cofrancesco, Drug-excipient compatibility studies by physico-chemical techniques. The case of atenolol, *J. Therm. Anal. Calorim.* 73 (2003) 547–561.
- [80] A. Ikeda, A. Takemura, H. Ono, Preparation of low-molecular weight alginate acid by acid hydrolysis, *Carbohydr. Polym.* 42 (2000) 421–425.
- [81] R. Vehring, Pharmaceutical particle engineering via spray drying, *Pharm. Res.* 25 (2008) 999–1022.
- [82] Y. Sugiyama, R.J. Larsen, J.-W. Kim, D. Weitz, Buckling and crumpling of drying droplets of colloid-polymer suspensions, *Langmuir* 22 (2006) 6024–6030.
- [83] M. Krantz, H. Zhang, J. Zhu, Characterization of powder flow: static and dynamic testing, *Fundam. Technol.* 194 (2009) 239–245.
- [84] L. Tajber, O.I. Corrigan, A.M. Healy, Spray drying of budesonide, formoterol fumarate and their composites-II. Statistical factorial design and in vitro deposition properties, *Int. J. Pharm.* 367 (2009) 86–96.

- [85] M.J. Donovan, H.D.C. Smyth, Influence of size and surface roughness of large lactose carrier particles in dry powder inhaler formulations, *Int. J. Pharm.* 402 (2010) 1–9.
- [86] Atenolol, in: S. Budavari (Ed.), *The Merck Index*, twelfth ed., Merck and Co., Inc., 1996, p. 892.
- [87] A. Rachocki, K. Pogorzelec-Glaser, C. Pawlaczyk, J. Tritt-Goc, Morphology, molecular dynamics and electric conductivity of carbohydrate polymer films based on alginic acid and benzimidazole, *Carbohydr. Res.* 346 (2011) 2718–2726.
- [88] M. Van Oort, In vitro testing of dry powder inhalers, *Aerosol Sci. Technol.* 22 (1995) 364–373.